A Sub-1 µW Multiparameter Injectable BioMote for Continuous Alcohol Monitoring

Haowei Jiang,* Xiahan Zhou,* Saurabh Kulkarni, Michael Uranian, Rajesh Seenivasan, and Drew A. Hall
Department of Electrical and Computer Engineering
University of California, San Diego
La Jolla, CA, USA
Email: drewhall@ucsd.edu

***Abstract*—This paper presents a wireless, fully-integrated, miniature "BioMote" sensor node that can be injected through a 16-gauge syringe for continuous, long-term alcohol monitoring. A microelectrode electrochemical sensor array that measures alcohol, background, and pH was implemented to differentially measure ethanol while removing interference and motion artifacts. The low-power multi-technique potentiostat supports both amperometric and potentiometric techniques achieving 2.5 nA sensitivity with 30.1 dB dynamic range and 0.5 mV sensitivity with 43 dB dynamic range, respectively. The measurements are transmitted to a wearable device through backscatter using a self-oscillating current-to-frequency (*I*-to-*F*) converter. The system is wirelessly powered via the coupling between an on-chip 4-turn coil and a wearable device at 985 MHz. The self-contained 0.85×1.5 mm² chip is implemented in 65 nm CMOS and consumes 970 nW.**

I. Introduction

Alcoholism is a widely prevalent disease affecting over 15 million adults and is the third leading cause of mortality in the United States [1]. Blood alcohol measurement plays an important role in forensic medicine and is a critical tool in substance abuse treatment programs to reduce relapse rates. The focus of this work is on the latter, where routine, unobtrusive monitoring is needed. Conventional sampling methods include breath analyzers and blood testing. The former requires user initiation and has limited correlation with the actual blood alcohol content (BAC) [2-3] whereas the latter must be collected by a trained professional and analyzed in a clinical laboratory. New techniques such as tattoo-based sensors are promising, but are easily removed and single-use only [2].

This paper presents a miniature, implantable, wireless alcohol sensor, a BioMote, that is subcutaneously injected into interstitial fluid (ISF), the quasi-stationary extracellular fluid surrounding cells composed of nutrients, metabolites, and waste. ISF is highly correlated with actual BAC enabling continuous, long-term biomarker monitoring. The system architecture is illustrated in Fig. 1 where power is wirelessly harvested from a wearable device, obviating the need for a bulky battery. A 4-turn on-chip coil (Q=10, L=40 nH) was implemented using the top metal layer of a 1P9M CMOS process. A 700 fF MIM cap, C_{in}, resonates the coil at 985 MHz, a frequency that was chosen based on the link efficiency and tissue compatibility [4]. A 5-stage self-synchronous full-wave rectifier converts the received RF power to a DC voltage, with a diode clamp at the output to prevent overvoltage conditions [5]. A bandgap reference and

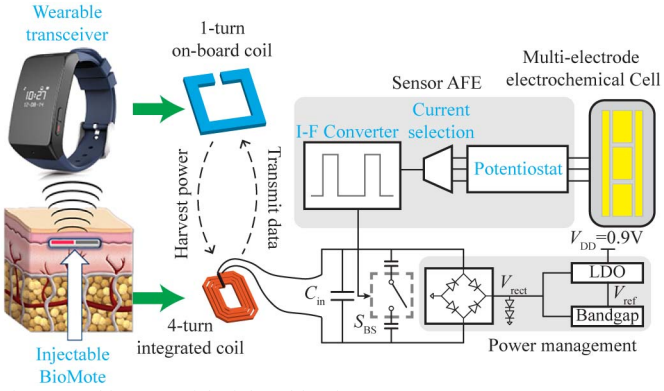

Fig. 1. Architecture of the injectable BioMote sensor.

LDO generate a regulated 900 mV supply voltage and 5 nA reference current. The microelectrode electrochemical sensors were placed inside of the on-chip coil also on the top metal layer, but without passivation and electroless plated with gold. The sensors are connected to a low-power potentiostat capable of performing both amperometric (for the alcohol and background measurements) and potentiometric (for the pH measurement) techniques. The dynamic range of the potentiostat was designed to cover only the necessary physiological range of alcohol and pH, thus saving power. The output of the potentiostat is fed into an *I*-to-*F* converter and transmitted via backscatter by modulating the resonant frequency of the wireless link.

Since the BioMote is wirelessly powered by a battery-powered device (e.g., a smartwatch), it is crucial to reduce the energy consumption. Thus, both the power draw of the circuits and the measurement time must be minimized. To achieve this: 1) A low-power potentiostat with a current-control loop and current-starved amplifier were designed that consumes only 500 nW, 2) The assay was designed to reduce the measurement time to 3 seconds, thus consuming just 3 µJ/measurement, and 3) Data are serially transmitted back to the wearable device through backscatter removing the need for an on-chip clock generator and ADC [5-6]. These techniques result in the first reported sub-1 µW fully integrated, wireless implantable sensor.

The rest of the paper is organized as follows: the sensing principle and assay are presented in Section II followed by the implementation of the circuits in Section III. Section IV presents electrical and *in-vitro* biological measurements results followed by a conclusion in Section V.

*H.J. and X. Z. contributed equally to this work.

This work is partially supported by the National Science Foundation (1621825), the National Institute of Health (R41DA044905), and Samsung.

978-1-5386-2483-8/18/$31.00 ©2018 IEEE

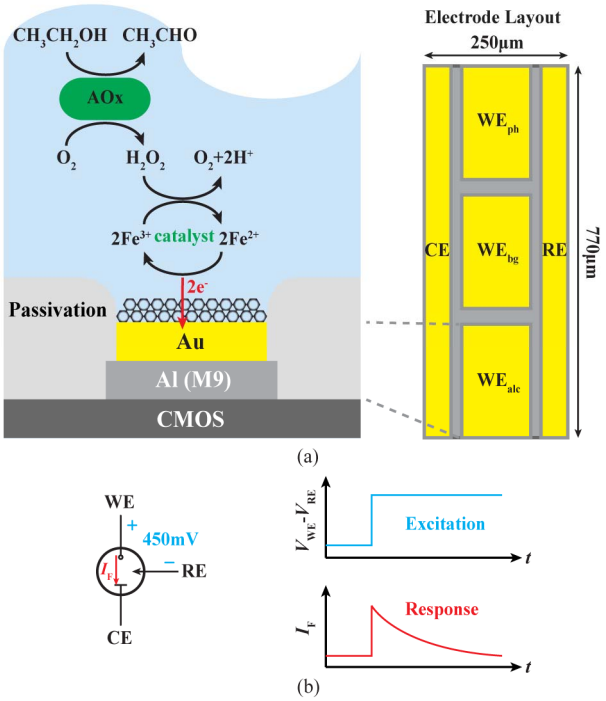

Fig. 2. (a) Illustration showing the alcohol assay and microelectrode layout, and (b) chronoamperometry measurement technique.

II. Sensing Principle

The sensing principle is based on an enzymatic reaction that occurs when alcohol oxidase (AOx) interacts with ethanol producing a hydrogen peroxide (H_2O_2) byproduct (Fig. 2a). Like a glucometer, the H_2O_2 byproduct is oxidized (by iron oxide nanoparticles in this work) to generate free electrons that are detected by the underlying gold-plated microelectrode. The iron oxide nanoparticles are imbedded in a polypyrrole (PPy) film on the surface of the sensor to facilitate efficient electron transfer and improve the sensitivity [7]. The reaction is quantified using chronoamperometry (Fig. 2b) where a 450mV step is applied between the working electrode (WE) and a reference electrode (RE) while measuring the resulting signal current that flows from the WE to the counter electrode (CE). The current response is determined by the Cottrell equation

$$I_F(t) = \frac{nFAC_0\sqrt{D_0}}{\sqrt{\pi t}}, \qquad (1)$$

where I_F is the signal current, n is the number of electrons transferred per interaction (2 in this assay), F is the Faraday constant, A is the area of the electrode, C_0 is the initial concentration of the reducible analyte, D_0 is the diffusion coefficient, and t is time. The equation shows that while a small area electrode design is desired for implantable biochips, the signal amplitude is linearly dependent on the area. Thus, the small integrated electrode requires a low-noise potentiostat.

It is well known that electrochemical measurements are sensitive to environmental perturbations such as temperature drift, mechanical movement, and pH variation. A multi-microelectrode architecture, which consists of three electrochemical sensors, is used to overcome this problem. One sensor is functionalized with the AOx enzyme to measure ethanol; the second sensor is unfunctionalized to measure background and non-specific/interfering species; and the third microelectrode is functionalized with a hydrogen ion selective membrane, iridium oxide (IrOx), to measure the pH. By subtracting the background from the functionalized electrode, common-mode signals are removed. The pH is used to digitally correct the measured ethanol concentration according to the Nernst equation. Each sensor has a separate WE with a shared reference RE and CE, all of which are created by electroless deposition of gold on openings in the top metal after fabrication. The RE is then subsequently covered with a silver paste.

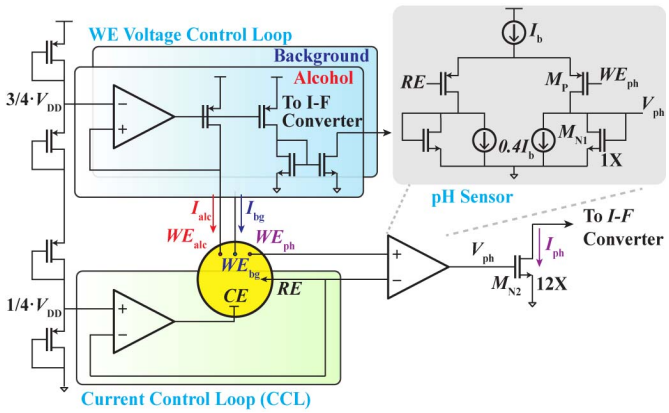

Fig. 3. Schematic of the multi-function potentiostat.

III. Circuit Implementation

A. Potentiostat

A low-power multi-function potentiostat was designed to support both chronoamperometry for the ethanol and potentiometry for the pH measurements (Fig. 3). A WE voltage control loop is used to bias the WE's at $3/4{\cdot}V_{DD}$ and a current mirror creates a copy of the current for the I-to-F converter. Since two WE's need to be measured separately, two WE control loops are required. A shared current control loop (CCL) biases the RE at $1/4{\cdot}V_{DD}$ to maintain a constant voltage difference ($1/2{\cdot}V_{DD}$) between the WE's and RE where the enzymatic reaction occurs. The signal currents I_{alc} and I_{bg} flow from WE_{alc} and WE_{bg} to CE respectively, and are limited by the CCL, which sets the maximum current at 80 nA to reduce unnecessary power consumption during start-up. The maximum current is determined by the physiological level of ethanol, which ranges from 2.17-43.4 mM (0.01-0.2 %BAC). This covers the range from no impaired behavior to loss of consciousness for typical adults.

The pH readout circuit consists of a current starved diode connected differential transconductance amplifier where the amplifier was sized to minimize the input-referred $1/f$ noise and have high input impedance. A change in solution pH induces a voltage on WE_{ph} that is then converted to a current by g_{mp} (the transconductance of transistor M_P) and amplified by 12× from M_{N2} to M_{N3}. Part of the tail current (80%) is siphoned off to enable a 5× reduction in power. Like the potentiostat, the overall transconductance (1.2 µS) is matched to the physiological range (pH 6.8 – pH 7.4) in ISF and the full-scale range of the I-to-F converter (120 nA).

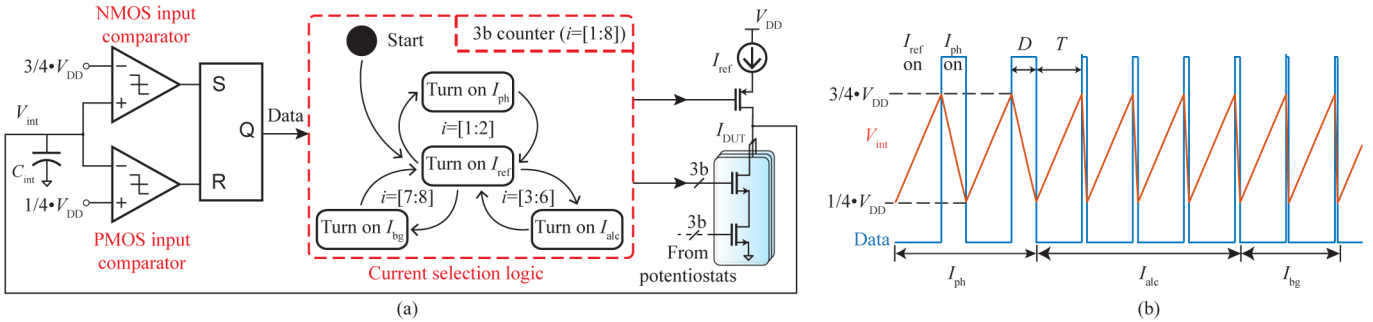

Fig. 4. (a) Schematic of the *I*-to-*F* converter and current selection logic, and (b) timing diagram of the current selection logic.

B. *I-to-F Converter*

The potentiostat output currents are mirrored to isolate the sensor from kickback and injected into an *I*-to-*F* converter, which translates the current amplitude into a frequency/duty cycle modulated waveform suitable for backscatter. Digitization is performed on the wearable device to reduce power and area. As shown in Fig. 4, a reference current, I_{ref}, charges a capacitor, C_{int}, until V_{int} exceeds a threshold voltage ($3/4 \cdot V_{DD}$) and triggers the NMOS input comparator to flip the SR-latch output. Next, one of the three sensor currents, I_{DUT}, is selected to discharge C_{int} until V_{int} drops below the lower threshold voltage ($1/4 \cdot V_{DD}$). The duty cycle, D, and period, T, of the *I*-to-*F* converter output are

$$D = \frac{V_{DD} C_{int}}{2 I_{DUT}}, \tag{2}$$

$$T = \frac{V_{DD} C_{int}}{2 I_{ref}}. \tag{3}$$

As such, I_{DUT} can be obtained with respect to I_{ref} by calculating the T/D ratio according to (2) and (3) without precisely needing to know the values of C_{int} or V_{DD} [8]. To minimize the efficiency loss due to backscatter operation, I_{ref} was chosen to be 5 nA, much less than I_{DUT}, and thus D < 20%. The comparator bandwidth was designed to be >50 kHz to minimize error from comparator delay for the narrowest pulse width (50 µs). Since there is no oscillator to clock the digital logic, a self-oscillating state-machine sequentially cycles through the I_{DUT} currents. A 3b divider driven by the *I*-to-*F* output divides the measurement period into 8 cycles, where I_{alc} is measured four times, while I_{bg} and I_{ph} are each measured twice (Fig. 4b). The 8-cycle measurement repeats continuously to reduce the noise through averaging and provide a distinct signature to distinguish the three I_{DUT}'s at the receiver without any synchronization. Using custom subthreshold digital logic gates, the state-machine consumes only 300 pW.

C. *Backscatter*

The *I*-to-*F* converter drives a backscatter switch, S_{BS}, (Fig. 1) that modulates the rectifier input impedance and thus the output voltage of the transmitter. When S_{BS} is on, two 1 pF MIM capacitors are connected in series and the resonant frequency shifts down to ~800 MHz. In simulation, this translates into 0.4% carrier tone amplitude change at 10 mm separation that can be detected by the transmitter. The backscatter also causes glitches on the rectifier output, V_{rect}, that are smoothed and attenuated by the LDO. By moving the power burden of transmitting data from the BioMote to the wearable device, the total power consumption is greatly reduced.

IV. Measurement Results

A. *Electrical Measurement Results*

A 1-turn coil (8×8 mm^2) fabricated on a Rogers 4350 substrate was placed on top of the sensor and with a varactor to resonate the coil at 985 MHz. The sensor was able to sustain a stable 0.9 V supply with a 2.4 mm thick pork loin chop at 18.5 dBm output power. Fig. 5(a) shows transient measurement results during startup for V_{rect} and the LDO output, V_{DD}, demonstrating successful wireless power delivery with a startup time less than 150 ms. Backscatter measurements taken from the output of the *I*-to-*F* and received using a direct down-conversion AM receiver with a passive mixer are shown in Fig. 5(b). The waveform was correctly recovered, and the 8-cycle pattern is clearly visible. It was found that the carrier tone amplitude change was only 0.2%, lower than simulation, likely because of a lower Q of the on-chip coil. Fig. 5(c) shows the measured potentiostat linearity with a 30.2 dB dynamic range (2.5-80 nA) in amperometry mode and a 43 dB dynamic range (0.5-70 mV) in potentiometry mode. The measured input-referred noise was 1.24 nA_{RMS} and 0.25 mV_{RMS}, respectively, which sets the lower limit while the CCL clamps the upper limit. Fig. 5(d) depicts the linear response between the potentiostat output current and the measured T/D ratio.

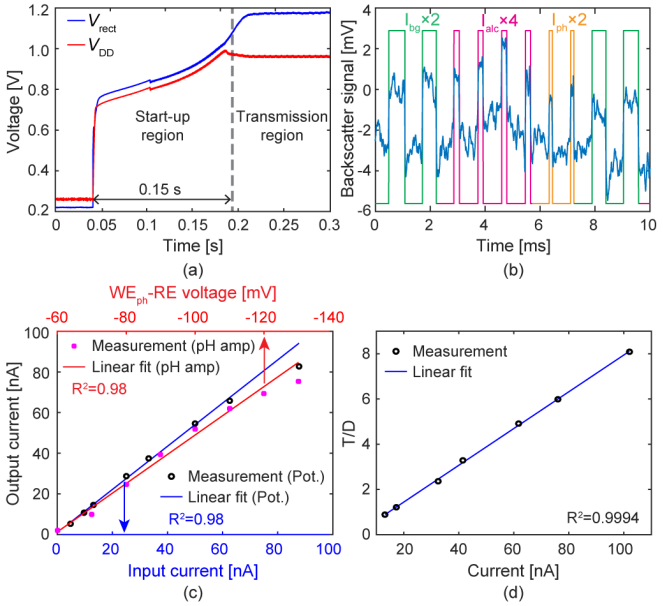

Fig. 5. Measured (a) transient voltage for wireless power transfer startup, (b) backscatter received output (blue) and *I*-to-*F* converter output, (c) potentiostat transfer curve, and (d) *I*-to-*F* converter transfer curve.

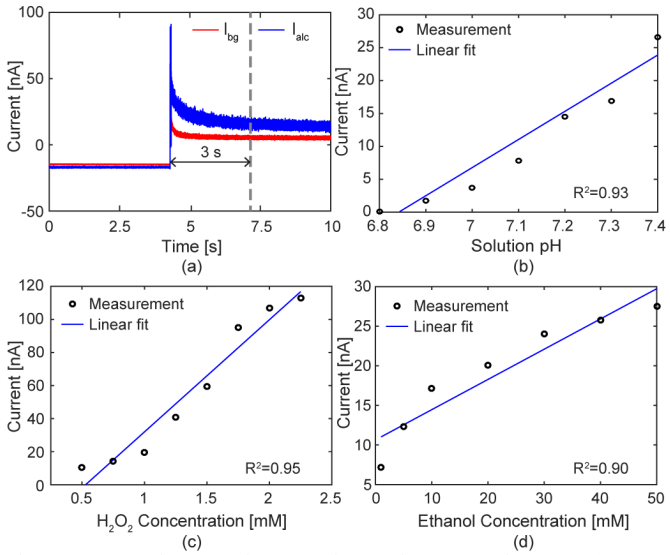

Fig. 6. Measured (a) transient waveforms, (b) pH transfer curve, (c) H_2O_2 transfer curve, and (d) ethanol transfer curve.

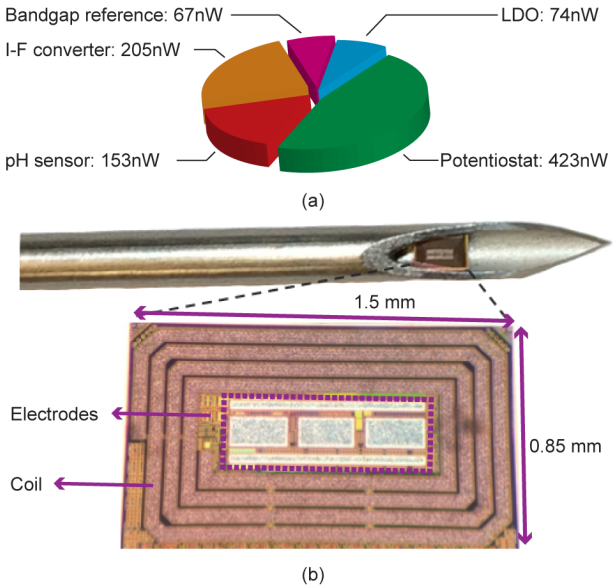

Fig. 7. (a) Simulated power breakdown and (b) annotated die photo.

B. Biological Measurement Results

in-vitro measurements were conducted to validate the performance of the chip and assay. Fig. 6(a) shows the time domain response of a single chronoamperometry measurement. One can see that the high startup current spike has been correctly limited by the CCL in the potentiostat. Fig. 6(b) shows the transfer curve from solution pH to I_{ph}, covering the proper pH range (6.8 to 7.4) in ISF. Fig. 6(c) and (d) show aggregated results for different concentrations of H_2O_2 and ethanol, respectively. The alcohol assay has a measured linear range of 1-50 mM corresponding to 0.0046-0.23 %BAC.

Table I summaries the performance of this work and compares it against state-of-the-art wireless implantable sensors. The power break-down is shown in Fig. 7(a). Figure 7(b) shows the die within a 16-gauge syringe.

TABLE I
PERFORMANCE COMPARISON OF IMPLANTABLE WIRELESS SENSORS

Parameter	[8]	Liao JSSC'12	[5]	[6]	Agarwal VLSI'17	This Work
Tech. (nm)	180	130	180	180	65	65
Carrier Freq. (MHz)	13.56	1,800	915	13.56	900	985
Supply (V)	1.8	1.2	1.2	1.8	1	0.9
Power (µW)	198	3	6	1,500	4	0.97
Sensitivity (nA)	1	2	12[1]	13	0.1	2.5 (alc.) 0.5 mV (pH)
Dynamic Range (dB)	60	37	32	48	71	30.1 (alc.) 43 (pH)
Size (mm)	4×8	10 (diameter)	1.4×1.4	12×12	1.2×1.2	0.85×1.5
Detection Technique	Amp.[2]	Amp.[2]	Amp.[2] + Volt.[3]	Amp.[2] + Volt.[3]	Amp.[2]	Amp.[2] + Volt.[3]
Analyte	Glucose	Glucose	Glucose	APAP	H_2O_2	Ethanol/H_2O_2
Multi-parameter?	No	No	No	BG[4]	No	BG[4] + pH
External Components	Sensor, coil, capacitor	Sensor, coil	None	Sensor, coil, capacitor	None	None

[1] Read from figure
[2] Amperometry
[3] Potentiometry
[4] Background

V. CONCLUSION

A wireless, fully-integrated injectable alcohol BioMote was designed for continuous, long-term monitoring. A micro-electrode sensor array and multi-function potentiostat enable differential measurements to cancel background interference, pH drift, and motion artifacts. Due to the low-power potentiostat, the system consumes state-of-the-art 970 nW power consumption and has all components integrated on a single 0.85×1.5 mm^2 chip.

ACKNOWLEDGMENT

The authors thank Li Gao for technical discussions about electromagnetic design, Alexander Sun for help with electrode plating, and CARI Therapeutics for market discussions.

REFERENCES

[1] "Alcohol Facts and Statistics | National Institute on Alcohol Abuse and Alcoholism (NIAAA)." [Online]. Available: https://www.niaaa.nih.gov/alcohol-health/overview-alcohol-consumption/alcohol-facts-and-statistics. [Accessed: 01-Nov-2017].

[2] J. Kim, *et al.*, "Noninvasive Alcohol Monitoring Using a Wearable Tattoo-Based Iontophoretic-Biosensing System," *ACS Sens.*, vol. 1, no. 8, pp. 1011–1019, Aug. 2016.

[3] T. D. Ridder, *et al.*, "Comparison of spectroscopically measured tissue alcohol concentration to blood and breath alcohol measurements," *J. Biomed. Opt.*, vol. 14, no. 5, 2009.

[4] S. O'Driscoll, *et al.*, "A mm-sized implantable power receiver with adaptive link compensation," in *ISSCC*, 2009, p. 294–295,295a.

[5] M. H. Nazari, *et al.*, "An implantable continuous glucose monitoring microsystem in 0.18 µm CMOS," in *Symposium on VLSI*, 2014, pp. 1–2.

[6] E. G. Kilinc *et al.*, "A System for Wireless Power Transfer and Data Communication of Long-Term Bio-Monitoring," *IEEE Sens. J.*, vol. 15, no. 11, pp. 6559–6569, Nov. 2015.

[7] S.-S. Lin and M. D. Gurol, "Catalytic Decomposition of Hydrogen Peroxide on Iron Oxide: Kinetics, Mechanism, and Implications," *Environ. Sci. Technol.*, vol. 32, no. 10, pp. 1417–1423, May 1998.

[8] M. M. Ahmadi and G. A. Jullien, "A Wireless-Implantable Microsystem for Continuous Blood Glucose Monitoring," *IEEE Trans. Biomed. Circuits Syst.*, vol. 3, no. 3, pp. 169–180, Jun. 2009.